Journal for Geometry and Graphics
Volume 22 (2018), No. 2, 283–299.

Spherical Geometry and Spherical Tilings with GeoGebra

Ana Maria D'Azevedo Breda[1], **José Manuel Dos Santos Dos Santos**[2]

[1] *Departamento de Matemática, Universidade de Aveiro*
Campus Universitário de Santiago, 3810-193 Aveiro, Portugal
email: ambreda@ua.pt

[2] *Universidade Aberta*
Rua da Escola Politécnica 141–147, 1269-001 Lisboa, Portugal
email: dossantosdossantos@gmail.com

Abstract. The classification of spherical tilings is a problem far from being solved. Here we show how to generate new families of antiprismatic spherical tilings using *GeoGebra*, a well known free software commonly used as a tool to teach and learn mathematics. Within the described propose some spherical geometry capabilities of *GeoGebra* had to be extended. The outline of the algorithms behind some of the newly designed and implemented *GeoGebra* tools and applications will be given.

Key Words: Spherical Geometry, Spherical Tilings, *GeoGebra*

MSC 2010: 51M20, 52C20, 05B45, 51N30, 97N80

1. Introduction

The research work described here has as its main goal a systematic way to generate spherical tilings and to search for new ones by making use of computational capabilities. Our main result is the description of the combinatorial and geometric characterisation of the spherical tiling family $\widehat{\mathfrak{B}_{\frac{p}{q}}}$, p, q in $\mathbb{N}$ with $\gcd(p, q) = 1$, which expands the antiprismatic spherical tilings.

The obtained results emerged by the new produced *GeoGebra* tools and the dynamic interaction capabilities of this software [18, 19], being the construction of an algorithm to get the orbit of a set of spherical points under the action of a (sub)group of spherical isometries (for the details see Section 2.4) as crucial point.

Let us consider the sphere centred at the point $O = (0, 0, 0)$, $S^2 = \{(x, y, z) \in \mathbb{R}^3 : d((x, y, z), (0, 0, 0)) = 1\}$. An element of S^2 is called a *spherical point*. Two spherical points are said to be *antipodal* points if the spherical distance between them is π.

ISSN 1433-8157/\$ 2.50

Any two non-antipodal spherical points, A and B, define uniquely a great circle, a *spherical line* s, on the sphere such that $A, B \in s$. The spherical line s will be also denoted by AB. The smaller of the two great arc circles terminated by A and B is called a *spherical segment* and denoted by $[AB]$.

Given a spherical segment $[AB]$, its *length* $|AB|$ is the measure of the angle $\angle AOB$, i.e., $|AB| = A\hat{O}B$. Given two spherical segments $[AB]$ and $[BC]$, they form a *spherical angle* $\widehat{ABC}$ defined by the angle between the tangent lines to the great circles AB and BC.

Considering three non-collinear spherical points on S^2, they define three spherical segments which bound two spherical regions. The smallest of these regions is the convex *spherical triangle* defined by the points; the other region is a concave spherical triangle. In this work we are only interested in convex spherical triangles. A spherical *n-gon* is a closed polygonal spherical line.

By a *spherical tiling* we mean a decomposition of the sphere by classes of congruent polygons (tiles). A *monohedral* spherical tiling is one in which all the tiles are congruent among them. In an monohedral spherical tiling any tile can be considered a prototile of the tiling. A *dihedral* spherical tiling is a tiling composed by two classes of congruent polygons, which means, a tiling made of two distinct prototiles. Similarly, *n-hedral* tilings, $n \in \mathbb{N}$ and $n \geq 3$, are tilings with n distinct prototiles.

There are many tools to work with spherical geometry as *Povray* [11], and in an interactive way *Sphaerica* [17] and *Spherical Easel* [1]. While *Povray* [17] is a powerful tool to illustrate objects in spherical geometry, *Sphaerica* and *Easel* present some potential to make constructions and explorations. For our purposes we need to work with more flexible tools and commands, in particular, we need to obtain in real time the orbit of a set of spherical points under the action of a (sub)group of spherical isometries. For that, *GeoGebra* [20] seems the best option for two crucial reasons: the widespread use of *GeoGebra* and the possibility of interaction with geometrical and algebraic representations simultaneously. In fact, *GeoGebra* has several geometrical representations in 2 and 3 dimensions allowing the interaction with spherical points in a diversity of ways. Besides, the algebraic capabilities of *GeoGebra* allow the study and the induction of some geometrical properties which may be visualized in real time. Among its many features, *GeoGebra* allows the creation of new tools and commands[1], deals with sequences of several geometrical and algebraic objects and uses logic procedures and heuristics which, among other things, permits one, for instance, to certify the congruence of objects. There are other software as powerful as *GeoGebra* for work in three-dimensional geometry (for example, *Archimedes Geo3D*[2]), but they are not free, and this is, without any doubt, an added value to the choice of *GeoGebra*. It is worthwhile to mention that this methodology (making use of *GeoGebra* tools) was already implemented in the exploration of planar hyperbolic tilings (see [26]).

The systematized study of spherical tilings started with D. Sommerville [24] who has established part of the classification of spherical tilings by isosceles triangles having analyzed a very particular case by scalene triangles [12, p. 467]. H. Davies in [9] presents an incomplete classification of triangular monohedral tilings of the sphere [9] omitting many details which were fixed lateron.

Tilings of the sphere by rectangular triangles were obtained by Yukako Ueno and Yoshio Agaoka in 1996 [29]. Later, in 2002, the same authors obtain the complete classification of monohedral edge-to-edge triangular spherical tilings [30]. Triangular spherical folding tilings

[1]For more details about tools in *GeoGebra* see [25, pp. 89–94] and [28].

[2]`http://spatialgeometry.com/drupal/en`

were studied by Ana Breda, and their classification was obtained in 1992, being these a subset of the triangular monohedral spherical tilings [7]. Spherical tilings by isosceles and right triangles can be found in [10, 13]. Recently, the authors using the tools described here, characterised a family of spherical monohedral tiles by four congruent and non-convex spherical pentagons [4].

The classification of spherical tilings by triangles is not yet completed. In fact, little is known when the condition of being monohedral or edge-to-edge is dropped out. A systemized study to enumerate and classify all spherical tilings is far from been solved.

Being a rich research field with several distinct ways of approach, tiling problems are interesting not only regarding theoretical aspects but also regarding the innumerable applications about the distribution of points on a sphere [23] with strong implications in the contemporary technology and in science in general. The study of spherical tiling has also applications to chemistry, for instance, in the study of periodic nanostructures [16], emerging new forms of association of molecules, notably fullerenes [15], which lead to the study of spherical tilings by triangles, squares, pentagons, and hexagons [21]. In the same line of reasoning other tilings including heptagons [27] and heptagon and octagons [22] had emerged. Some other research points to new possibilities for new molecular patterns [31, 14]. The facility location problems and spherical designs and minimal energy point configurations on spheres [2, 3] are other fields where the study of tilings can be used for which we may give some contributions.

Next, we begin, in Section 2, presenting some tools created that extend *GeoGebra* capabilities in spherical geometry. In Section 3, we introduce and prove our main results. Subsequently, in Section 4, we also explain other ways of obtaining spherical tilings, from a spherical triangle subject to the local action of a (sub) group of symmetries, a strategy that may help to find new spherical tilings. Finally, in Section 5, we present some of our conclusions about the use of *GeoGebra* in the study of spherical tilings.

2. GeoGebra tools for spherical geometry

GeoGebra gives the possibility of interacting, simultaneously, with graphic, algebraic and calculus views. It also gives the chance to create new tools and commands. In fact, the tools can be created from the combination of existing tools or commands. The new tool and the corresponding commands can be used in new constructions or may be integrated in the construction of new tools. We will use these functionality to construct useful tools and commands for spherical geometry. Next we will show how some of the new tools may be used.

2.1. Spherical geometry tools

Spherical *GeoGebra* tools were constructed for the purpose to explore, among others, spherical tilings. Among these spherical tools, we mention the following ones: *Spherical Segment*, *Spherical Equidistant Points*, *Spherical Compass*, *Spherical Equilateral Triangle*. Here, by way of example, we describe how the Spherical Segment tool was constructed.

Given two non antipodal spherical points A and B, the spherical segment joining them is a great circular arc bounded by A and B. These spherical segment can be obtained in *GeoGebra* using the command *SphereSegment[A,B]* described below (see Figure 1).

Tool Name	Spherical Segment
Command Name	SphericalSegment
Syntax	SphericalSegment[A,B]
Help	Given A,B and a spherical, s, draw the spherical segment joining A to B.
Icon	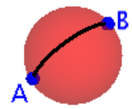
Script	s=Sphere[(0,0,0), 1] A=PointIn[s] B=PointIn[s] If[Distance[A,B]≠2,CircularArc[(0,0,0), A,B,Plane[(0,0,0),A,B]]]

Figure 1: Tool to construct a spherical segment.

2.2. Spherical geometry tool to construct a spherical triangle given three angles

It is well known that we may use trigonometric relations to obtain the arc lengths of a spherical triangle given the measurements of its spherical angles.

Let A, B and C be the vertices of a spherical triangle and α, β, γ the measure of the corresponding spherical angles. Denoting by a the measure of the arc BC, $a = |BC|$, b the measure of AC, $b = |AC|$, and c the measure of the arc AB, $c = |AB|$, the following relations hold:

$$\cos a = \cos\alpha + \frac{\cos\beta\cos\gamma}{\sin\beta\sin\gamma}, \quad \cos b = \cos\beta + \frac{\cos\alpha\cos\gamma}{\sin\alpha\sin\gamma}, \quad \cos c = \cos\gamma + \frac{\cos\alpha\cos\beta}{\sin\alpha\sin\beta}. \tag{1}$$

Thus, we may obtain the measure of the arcs, as a function of the angles of the spherical triangle. Using these proprieties we may create the tool, following the steps described below.

(i) Definition of the unit sphere:
$O = (0, 0, 0)$;
$S = Sphere[O, 1]$.
(ii) Defining three angles of the spherical triangle.
$\alpha = pi/2$;
$\beta = pi/2$;
$\gamma = pi/2$.
(iii) Creating the vertices A, B and C:
A=Point[IntersectPath[z = 0, S]]
B=Rotate[A, acos((cos(γ) + cos(α) cos(β)) / (sin(α) sin(β))), Centre[S], z = 0]
C=Intersect[IntersectPath[PerpendicularPlane[Rotate[A, acos((cos(β) + cos(α) cos(γ)) / (sin(α) sin(γ))),Centre[S], z = 0], Line[Centre[S], A]], S], IntersectPath[PerpendicularPlane[Rotate[Rotate[A, acos((cos(γ) + cos(α) cos(β)) / (sin(α) sin(β))),Centre[S], z = 0], acos((cos(α) + cos(β) cos(γ)) / (sin(β) sin(γ))), Centre[S], z = 0], Line[Centre[S], Rotate[A, acos((cos(γ) + cos(α) cos(β)) / (sin(α) sin(β))), Centre[S], z = 0]]], S], 1]
(iv) Drawing the edges of spherical triangle:
Sa=CircularArc[O,B,C];
Sb=CircularArc[O,A,C];
Sc=CircularArc[O,A,B].
(v) Creating The tool

The final step is the creation of the *GeoGebra* tool hiding all the constructions presented in the algebraic view, as illustrated in Figure 2.

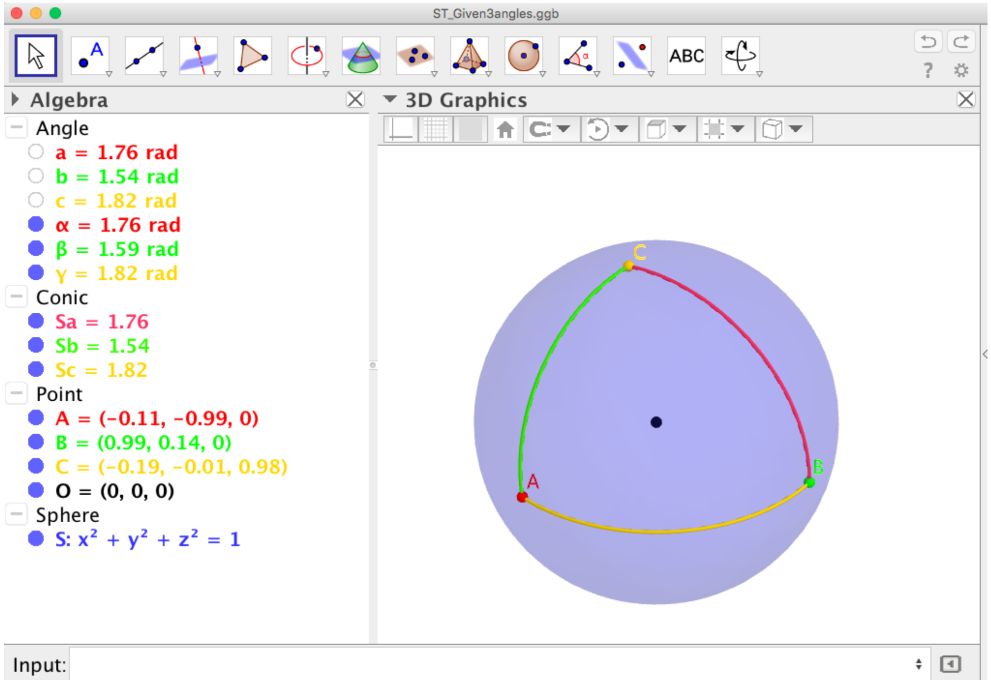

Figure 2: *GeoGebra* application to create a spherical triangle given three angles.

This tool is useful to find spherical tilings and search for new spherical patterns. These tool can be easily adapted to create tools to build any type of spherical triangles.

2.3. An application of the Equilateral Spherical Triangle Tool

One of the spherical tools constructed was the *Spherical Compass*. Using this tool we can easily construct equilateral spherical triangles.

Starting from a net of n congruent equilateral triangles, depending on initial points A and B, and moving these points around the sphere, we can explore many configurations where some of them are spherical tilings. In Figure 3 we illustrate these procedure, using nets with three, eight and twenty triangles ending up in the tetrahedral, octahedral and icosahedral regular spherical tilings. Using the same strategy with another net of triangles, for example with common vertices or adjacent sides, and observing the evolution of the set according to the different positions of the initial points, we may explore the possibilities to obtain new spherical tilings. The application presented above will be used and improved to develop some research in spherical tilings.

In the next section we show another way to find spherical tilings using spherical isometries.

2.4. Using spherical isometries to obtain spherical tilings by means of GeoGebra

Let s be the sphere centred in $O = (0, 0, 0)$ and radius 1. Let e be a great circle of s and A and B two distinct points in e. Choose one point $C \in s$ such that $[ABC]$ defines an equilateral triangle.

Let $\mathfrak{B}_n$, $n \in \mathbb{N}$, be a band (closed net) of n congruent spherical equilateral triangles. Using the tool *equilateral spherical triangle*, *SEqT[A,B]*, we can construct an application to explore some properties of the band $\mathfrak{B}_n$. We will start with $n = 12$ (see Figure 4).

This application works in a similar way to that shown in Figure 3. Its use (exploration) reveals that for each position of the point B:

Using a set of n equilateral triangles	...in one hemisphere	...closing around one vertex	final length of segment AB
3	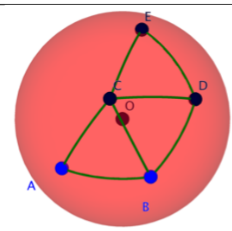	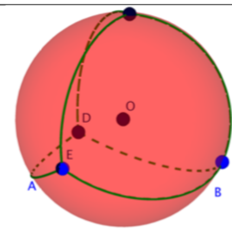	$\arccos(-\frac{1}{3}) = = 2\arctan(\sqrt{2}) \approx \approx 1.908\text{rad}$
8	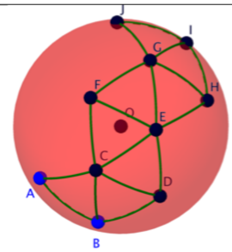	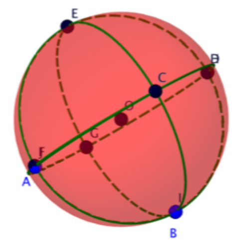	$\frac{\pi}{2} \approx 1.574\text{rad}$
20	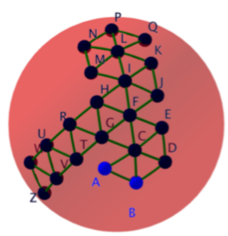	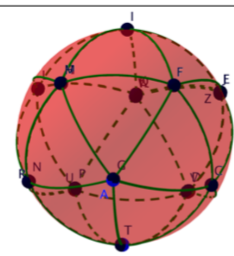	$2\arcsin(\frac{\sqrt{5-\sqrt{5}}}{\sqrt{10}}) \approx \approx 1.107\text{rad}$

Figure 3: Evolution of nets of equilateral and congruent triangles (see [6]).

i) the orbits of the points A and C leave in the same plane, α;
ii) the orbits of the point B are in a plane, β, parallel to α;

```
s:Sphere[(0,0,0),1]
e:IntersectPath[z=0,s]
A=(1,0,0)
B=Point[e]
ABC=CircularArc[(0,0,0),A,B,Plane[(0,0,0),A,B]],CircularArc[(0,0,0),B,C,Plane[(0,0,0),B,C]],
CircularArc[(0,0,0),C,A,Plane[(0,0,0),C,A]]
CBD=SEqT[C,B]
CDE=SEqT[C,D]
EDF=SEqT[E,D]
EFG=SEqT[E,F]
GFH=SEqT[G,F]
GHI=SEqT[G,H]
IHJ=SEqT[I,H]
IJK=SEqT[I,J]
KJL=SEqT[K,J]
KLM=SEqT[K,L]
MLN=SEqT[M,L]
```

Figure 4: *GeoGebra* commands to explore the orbit of the equilateral triangles in band $\mathfrak{B}_{12}$.

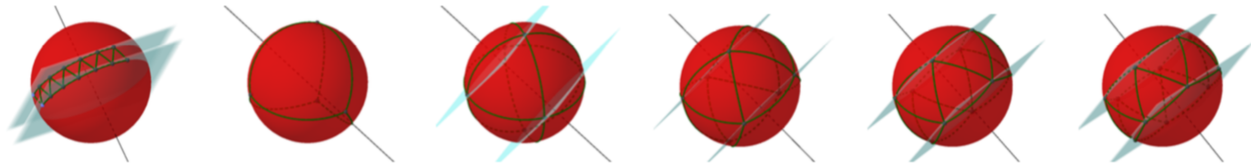

Figure 5: Band with 12 equilateral spherical triangles. Cases that end up in antiprismatic spherical tilings (see [5]).

iii) the distance between α and β is equal to the height of the spherical triangle $[ABC]$;
iv) for the values of the length of AB equal to $\frac{\pi}{2}+\arcsin\left(\frac{1}{3}\right)$, $\frac{\pi}{2}$, $\arccos\left(\frac{2\sqrt{2}-1}{7}\right)$, $\arccos\left(\frac{\sqrt{5}}{5}\right)$, $\arccos\left(\frac{\sqrt{3}}{3}\right)$ we obtain, respectively, the spherical tilings induced by the antiprisms of 4, 6, 10, 12 and 14 faces (see Figure 5).

The exploration of the above *GeoGebra* application revealed that the orbit of the triangle $[ABC]$ is generated by the action of a group of spherical rotations about an axis r, perpendicular to the plane α and β, passing through the center of s. Let P be the point of intersection of a and r. Then the band $(\mathfrak{B}_n)_{n\in\mathbb{N}}$ is obtained by rotations of the spherical triangle $[ABC]$ about the axis r by multiples of $\angle APB$.

For our purposes we are interested in knowing the conditions for which $\mathfrak{B}_n, n \in \mathbb{N}$, generates spherical tilings.

In order to construct a more accurate *GeoGebra* application to allow more generalized cases we consider

i) the sphere s, the north pole P_N=(0,0,1);
ii) natural numbers p and q, $q < p$, defined by sliders;
iii) the point B_1, in the north hemisphere of s;
iv) the point B_2 obtained by the rotation of B_1 about the z-axis by an angle of $2\pi/\frac{p}{q}$;
v) the point A_1, a point in the bisector of the arc B_1B_2, which not belong to this arc, that is, a point at the same spherical distance from B_1 and B_2 (note that A_1 belongs to the great circle defined by the plane $y = 0$).

Under these conditions, $[B_1B_2A_1]$ defines an equilateral spherical triangle. Denoting, respectively, by l and h the half of the length and the height of the spherical triangle $[B_1B_2A_1]$, chosen in the way described previously, one has

$$l = l\left(\frac{p}{q}\right) = \sqrt{2}\,\frac{\sqrt{\cos\left(\pi/\frac{p}{q}\right)+2\sin^2\left(\pi/\frac{p}{q}\right)+1}}{\cos\left(\pi/\frac{p}{q}\right)+2\sin^2\left(\pi/\frac{p}{q}\right)+1},\quad h = h\left(\frac{p}{q}\right) = \frac{\sqrt{\left(\cos\left(\pi/\frac{p}{q}\right)+2\sin^2\left(\pi/\frac{p}{q}\right)\right)^2-1}}{\cos\left(\pi/\frac{p}{q}\right)+2\sin^2\left(\pi/\frac{p}{q}\right)+1}.$$

Note that for l being well defined we need that $\cos\left(\pi/\frac{p}{q}\right)+2\sin^2\left(\pi/\frac{p}{q}\right)+1 \neq 0$, which corresponds to $\frac{p}{q} \neq \frac{1}{2n+1}$, $n \in \mathbb{N}$. [3]

On the other hand, for h being well defined we need that

$$\left(\cos\left(\pi/\frac{p}{q}\right)+2\sin^2\left(\pi/\frac{p}{q}\right)\right)^2-1 \geq 0.$$

[3] The application of *GeoGebra* shows the three points B_1, B_2 and A_1 coincident.

If $x := \cos\left(\pi/\frac{p}{q}\right)$ then $(-2x^2+x+2)^2-1 \geq 0 \iff -\frac{1}{2} \leq x \leq 1$. Thus, if $-\frac{1}{2} \leq \cos\left(\pi/\frac{p}{q}\right) \leq 1$ then $0 < q \leq \frac{2}{3}\,p$. Hence, h is well defined if and only if $\frac{p}{q} \geq \frac{3}{2}$.

Accordingly,

$$B_1 = \left(l\left(\tfrac{p}{q}\right)\cos\left(\pi/\tfrac{p}{q}\right),\ -l\left(\tfrac{p}{q}\right)\sin\left(\pi/\tfrac{p}{q}\right),\ h\left(\tfrac{p}{q}\right)\right),$$

$$B_2 = \left(l\left(\tfrac{p}{q}\right)\cos\left(\pi/\tfrac{p}{q}\right),\ l\left(\tfrac{p}{q}\right)\sin\left(\pi/\tfrac{p}{q}\right),\ h\left(\tfrac{p}{q}\right)\right), \qquad A_1 = \left(l\left(\tfrac{p}{q}\right),\ 0,\ -h\left(\tfrac{p}{q}\right)\right).$$

Therefore $[B_1B_2A_1]$ is an equilateral triangle with side lengths equal to

$$|B_1B_2| = |B_2A_1| = |A_1B_1| = \arccos\left(\frac{\cos\left(\pi/\frac{p}{q}\right) + 2\cos^2\left(\pi/\frac{p}{q}\right) - 1}{\cos\left(\pi/\frac{p}{q}\right) + 2\sin^2\left(\pi/\frac{p}{q}\right) + 1}\right),$$

$$|B_1B_2| = |B_2A_1| = |A_1B_1| = \arccos\left(\frac{1 - 2\cos\left(\pi/\frac{p}{q}\right)}{2\cos\left(\pi/\frac{p}{q}\right) - 3}\right),$$

and with an angle measure equal to

$$\widehat{B_1B_2A_1} = \widehat{B_2A_1B_1} = \widehat{A_1B_1A_2} = \arccos\left(-\frac{1}{2} + \cos\left(\pi/\frac{p}{q}\right)\right).$$

The orbit of the equilateral triangle $[B_1B_2A_1] \bigcup A_1A_2$ by the the action of a group of rotations about the z-axis and of angle $2\pi/\frac{p}{q}$, can be obtained using the *GeoGebra* commands defined in Figure 7.

The generated spherical patterns depend on the value of $\frac{p}{q}$. When $\frac{p}{q} \in \mathbb{N}$ and $\frac{p}{q} > 2$ the orbit defines spherical antiprisms associated to the $\frac{p}{q}$-gon antiprism. All vertices have equal valence $(3,\ 3,\ 3,\ \frac{p}{q} = n)$, and the tiling has $2n$ vertices, $4n$ edges, $2n$ spherical triangles and

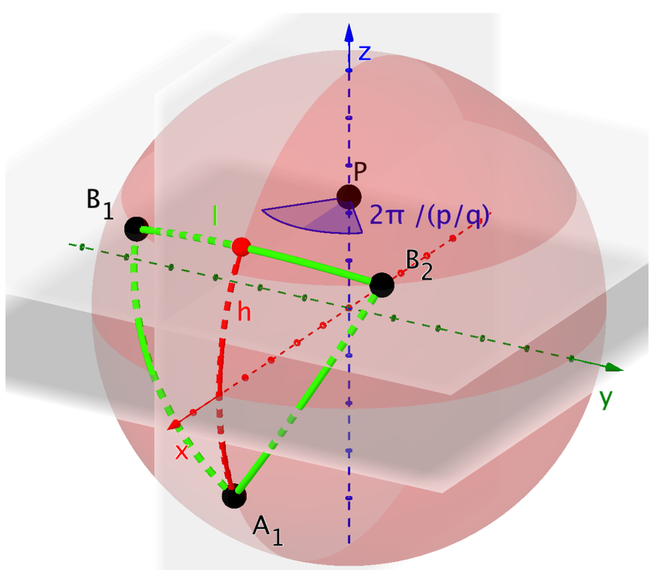

Figure 6: Spherical triangle $[B_1B_2A_1]$.

```
Sequence(Rotate(CircularArc((0,0,0),B1,B2,Plane((0,0,0),B1,B2)),k 2 pi/(p/q),zAxis),k,1,pq)
Sequence(Rotate(CircularArc((0,0,0),B2,A1,Plane((0,0,0),B2,A1)),k 2 pi/(p/q),zAxis),k,1,pq)
Sequence(Rotate(CircularArc((0,0,0),A1,B1,Plane((0,0,0),A1,B1)),k 2 pi/(p/q),zAxis),k,1,pq)
Rotate(Reflect(Sequence(Rotate(CircularArc((0,0,0),B_1,B_2,Plane[(0,0,0),B_1,B_2)),k 2 pi/(p/q),
zAxis),k,1,pq),Plane(z=0)),pi/(p/q),zAxis)
```

Figure 7: *GeoGebra* commands for the generation of spherical tilings.

2 spherical n-gons[4]. All the triangles have congruent angles of measure $\arccos\left(\cos\left(\frac{\pi}{n}\right)-\frac{1}{2}\right)$. The spherical n-gons have congruent angles with measure $2\pi - 3\arccos\left(\cos\left(\frac{\pi}{n}\right)-\frac{1}{2}\right)$. All arcs of these tilings have measure $\arccos\left((1-2\cos\left(\frac{\pi}{n}\right))/(2\cos\left(\frac{\pi}{n}\right)-3)\right)$. All these tiling are invariant by the cycled group of order n and have central symmetry.

Analysing the behaviour of the maps h and l and considering their domain as the set of real numbers, we can prove in a straightforward way that $\lim_{x\to\infty} l(x) = 1$ and $\lim_{x\to\infty} h(x) = 0$ which corresponds to the construction of a tiling of the sphere by two hemispheres. Considering $x > \frac{3}{2}$, the function h has a maximum of $\frac{3}{5}$ and l has a minimum of $\frac{4}{5}$ at $x = \pi/\arccos\left(\frac{1}{4}\right)$, thus the minimum value of $2l$ is $\frac{8}{5}$, near of the arc length of the prototype of the tetrahedral spherical tiling, corresponding to the tiling of the sphere by equilateral triangles.

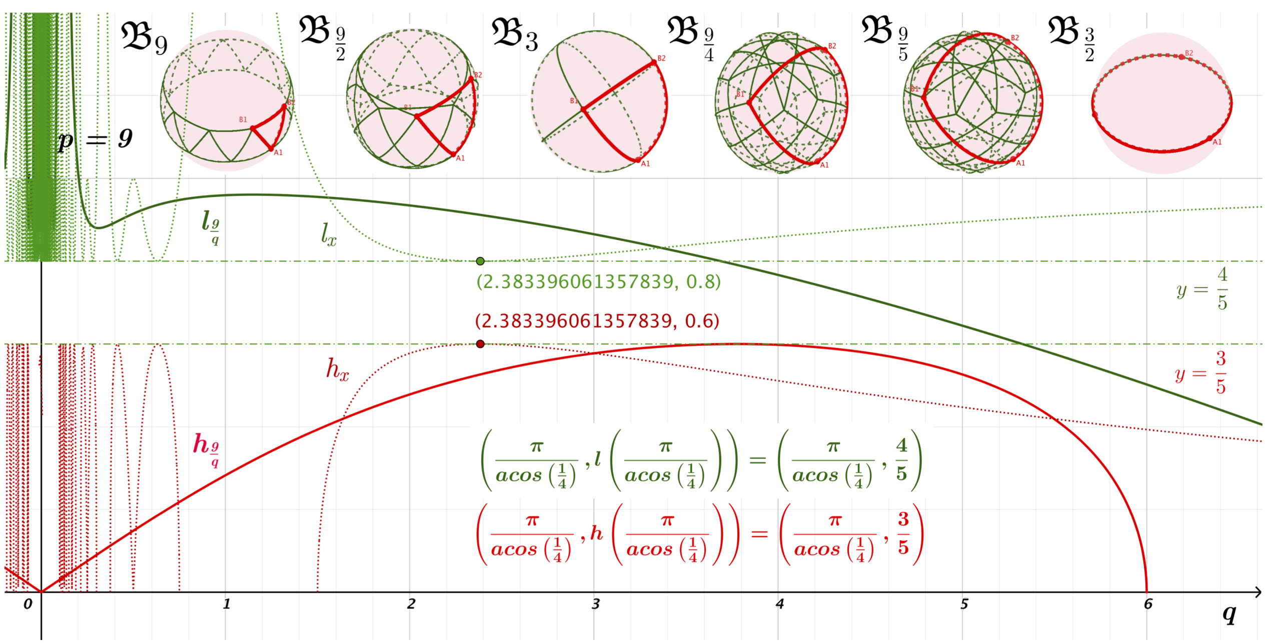

Figure 8: *GeoGebra* output of the graph behaviour of functions h and l, where $h_{\frac{9}{q}} = h(\frac{9}{q})$ and $l_{\frac{9}{q}} = l(\frac{9}{q})$.

If $\frac{3}{2} < x < \pi/\arccos\left(\frac{1}{4}\right)$ the corresponding side lengths B_1B_2 decrease to a minimum of $\frac{4}{5}$, while the sequence of heights of the corresponding triangles $[B_1B_2A_1]$ grow to a maximum value of $\frac{3}{5}$. Thus the generated bands, $\mathfrak{B}_x$, range from a set of two hemispheres to other bands whose "non-lateral" edges have their midpoints increasingly close to the poles (see Figure 8, $\mathfrak{B}_k$, $k \in \{\frac{3}{2}, \frac{9}{5}, \frac{9}{4}\}$).

[4]In this case the Euler formula, $F + V = E + 2$, is obviously satisfied. Note that the tilings induce the antiprism inscribed in the sphere.

Anti Prism Spherical tilings $\widehat{\mathfrak{B}_n}, n \in \mathbb{N}$	$\widehat{\mathfrak{B}_4}$ 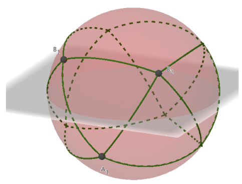	$\widehat{\mathfrak{B}_5}$ 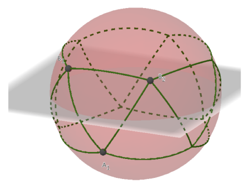	$\widehat{\mathfrak{B}_6}$ 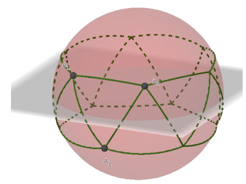
Planar Graph	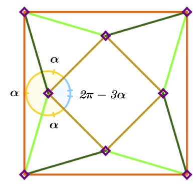	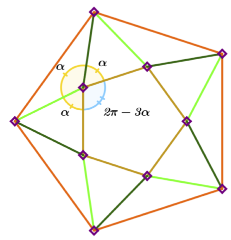	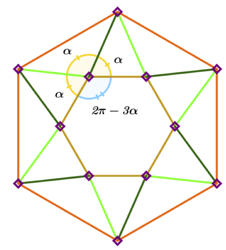
Vertices valence $(3,3,3,n)$	$(3,3,3,4)$	$(3,3,3,5)$	$(3,3,3,6)$
Angles around vertices $(\alpha;\alpha;\alpha;2\pi-3\alpha)$	$(\alpha;\alpha;\alpha;2\pi-3\alpha)$	$(\alpha;\alpha;\alpha;2\pi-3\alpha)$	$(\alpha;\alpha;\alpha;2\pi-3\alpha)$
$\alpha = \widehat{B_1B_2A_1}$ $\alpha = \arccos\left(cos\left(\frac{\pi}{n}\right)-\frac{1}{2}\right)$	$\arccos\left(\frac{\sqrt{2}-1}{2}\right)$	$\frac{2\pi}{5}$	$\arccos\left(\frac{1}{2}\ \left(\sqrt{3}-1\right)\right)$
$\arccos\left(\frac{1-2\cos\left(\frac{\pi}{n}\right)}{2\cos\left(\frac{\pi}{n}\right)-3}\right) = \lvert\widehat{B_1B_2}\rvert$	$\arccos\left(\frac{2\sqrt{2}-1}{7}\right)$	$\arccos\left(\frac{\sqrt{5}}{5}\right)$	$\arccos\left(\frac{\sqrt{3}}{3}\right)$
(Vertices, Edges, Faces) $(2n, 4n, 2n+2)$.	$(8, 16, 10)$	$(10, 20, 12)$	$(12, 24, 14)$

Figure 9: n-gon antiprism, $n \in \mathbb{N}$ and $n > 2$, obtained by rotations of a band of $2n$ equilateral triangles.

On the other hand, if $x > \pi/\arccos\left(\frac{1}{4}\right)$ the midpoints of the "non-lateral" edges of the band move away from the poles until the tiling pattern, associated with an regular n-agon antiprism is obtained (see Figure 8, $\mathfrak{B}_k$, $k \in \{3, \frac{9}{2}, 9\}$).

Figure 9 illustrates $\mathfrak{B}_n$, $n \in \{4,5,6\}$, and shows the arcs lengths, the angle measures and the planar configuration associated to the corresponding generated spherical tiling, from now on denoted by $\widehat{\mathfrak{B}_n}$. The angles and arcs measure of the triangles of the associated tilings can be obtained, dynamically, with the *GeoGebra* CAS.

By the use of the *sequence* command, *GeoGebra* uncovers more complex tilings as the ones illustrated in Figure 10, when we allow n to be the rational numbers $\frac{5}{q}$ with $q \in \{1,2,3\}$.

The tiling $\widehat{\mathfrak{B}_{\frac{5}{1}}}$ corresponds to the spherical pentagonal antiprism tiling described above. If $n = \frac{5}{2}$, the tiling $\widehat{\mathfrak{B}_n}$ has 25 vertices, 27 tiles from which two are spherical pentagons, ten are spherical triangle and fifteen are spherical quadrilaterals (five spherical rhombus and ten spherical kites). Finally, if $n = \frac{5}{3}$, the corresponding tiling $\widehat{\mathfrak{B}_{\frac{5}{3}}}$ has 30 vertices defining 32 tiles (two spherical pentagons, ten spherical triangles, and twenty spherical kites).

In Figure 10 we may observe the tilings $\widehat{\mathfrak{B}_{\frac{5}{q}}}$, $q \in \{1,2,3\}$. This figure highlights the rotational symmetry of order 5 about the x-axis of all these tilings, the central symmetry of

	$\widehat{\mathfrak{B}_{\frac{5}{1}}}$	$\widehat{\mathfrak{B}_{\frac{5}{2}}}$	$\widehat{\mathfrak{B}_{\frac{5}{3}}}$
Tilings	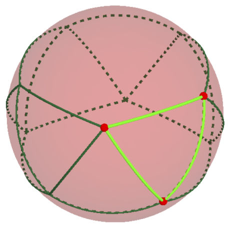	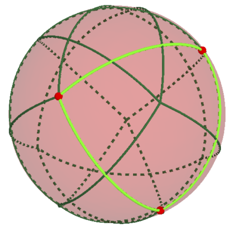	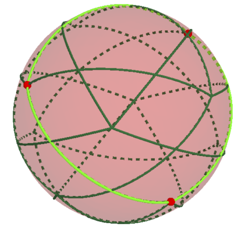
length of $\widehat{B_1B_2}$	$\arccos\left(\frac{\sqrt{5}}{5}\right)$	$\arccos\left(\frac{\sqrt{5}-4}{11}\right)$	$\arcsin\left(\frac{\sqrt{5}}{5}\right)+\frac{\pi}{2}$
Angles	$\frac{4\pi}{5};\frac{2\pi}{5}$	$\alpha=\arccos\left(\frac{1}{4}\left(\sqrt{5}-3\right)\right)$;$2\pi-3\alpha$	$\frac{\pi}{3};\frac{2\pi}{5};\frac{2\pi}{3};\frac{4\pi}{5}$
Vertices: valence; angles; number.	$(3,3,3,5)$; $(\frac{2\pi}{5},\frac{2\pi}{5},\frac{2\pi}{5},\frac{4\pi}{5})$; 10.	$(3,4,3,5)$; $(3,4,4,4)$; $(4,4,4,4)$; $(3,4,4,4)$; $(3,4,3,5)$; 5 groups of 5 vertices each, in a total of 25.	$(3,4,3,5)$; $(\frac{\pi}{3},\frac{2\pi}{3},\frac{\pi}{3},\frac{2\pi}{3})$; $(3,4,4,4)$; $(\frac{2\pi}{5},\frac{2\pi}{5},\frac{4\pi}{5},\frac{2\pi}{5})$; $(4,4,4,4)$; $(\frac{\pi}{3},\frac{2\pi}{3},\frac{\pi}{3},\frac{2\pi}{3})$; $(4,4,4,4)$; $(\frac{\pi}{6},\frac{\pi}{3},\frac{\pi}{6},\frac{\pi}{3})$; $(3,4,4,4)$; $(\frac{2\pi}{5},\frac{2\pi}{5},\frac{4\pi}{5},\frac{2\pi}{5})$; $(3,4,3,5)$; $(\frac{\pi}{3},\frac{2\pi}{3},\frac{\pi}{3},\frac{2\pi}{3})$; 6 groups of 5 vertices each, in a total of 30.
Polyhedron	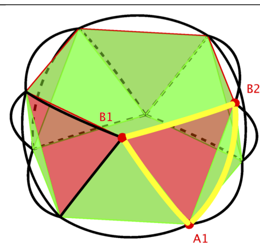	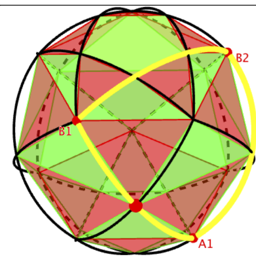	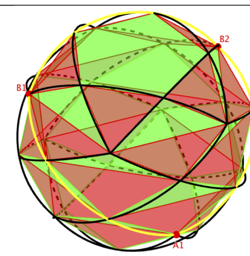
Faces Vertices Edges	12 Faces: 2, 5-gons; 2, 3-gons. 10 Vertices 20 Edges	37 Faces: 2, 5-gons; 30, 3-gons; 5, 4-gons. 25 Vertices 60 edges	42 Faces: 2, 5-gons; 40, 3-gons. 30 Vertices 70 edges

Figure 10: $\mathfrak{B}_{\frac{5}{q}}, q \in \{1,2,3\}$, combinatorial, geometric proprieties, and some of the associated polyhedra.

$\widehat{\mathfrak{B}_{\frac{5}{q}}}, q \in \{2,3\}$ and the reflection symmetry of $\widehat{\mathfrak{B}_{\frac{5}{2}}}$.

It should be noted that in this study we are not interested in the prismatic compound antiprisms, whose bases correspond to skew zig-zag polygons [8]. Although they appear in some cases, we emphasise that the tilings described above go beyond the class of tilings associated with those polyhedra. In our description there are tilings in which vertices of a given tile are not coplanar. This is the case of $\widehat{\mathfrak{B}_{\frac{5}{2}}}$ and $\widehat{\mathfrak{B}_{\frac{5}{3}}}$ (see Figure 10).

We may associate a polyhedron to these type of tilings, making use of a triangulation of the non-coplanar tiles, but the process is not unique. The tiling $\widehat{\mathfrak{B}_{\frac{5}{2}}}$ has 27 spherical faces, 25 vertices and 40 edges; and we may associated to this tiling several polyhedra with 37 faces, 25 vertices and 60 edges (see row five in the table illustrated in Figure 10). It is worthwhile to mention that, while the tiling $\widehat{\mathfrak{B}_{\frac{5}{2}}}$ has two types of quadrangular faces, one with coplanar vertices and other with not coplanar vertices, the tiling $\widehat{\mathfrak{B}_{\frac{5}{3}}}$ has all quadrangular faces of a single type; its vertices are always non-coplanar.

Let p and q be any two natural numbers, $p > q$. Observe that:

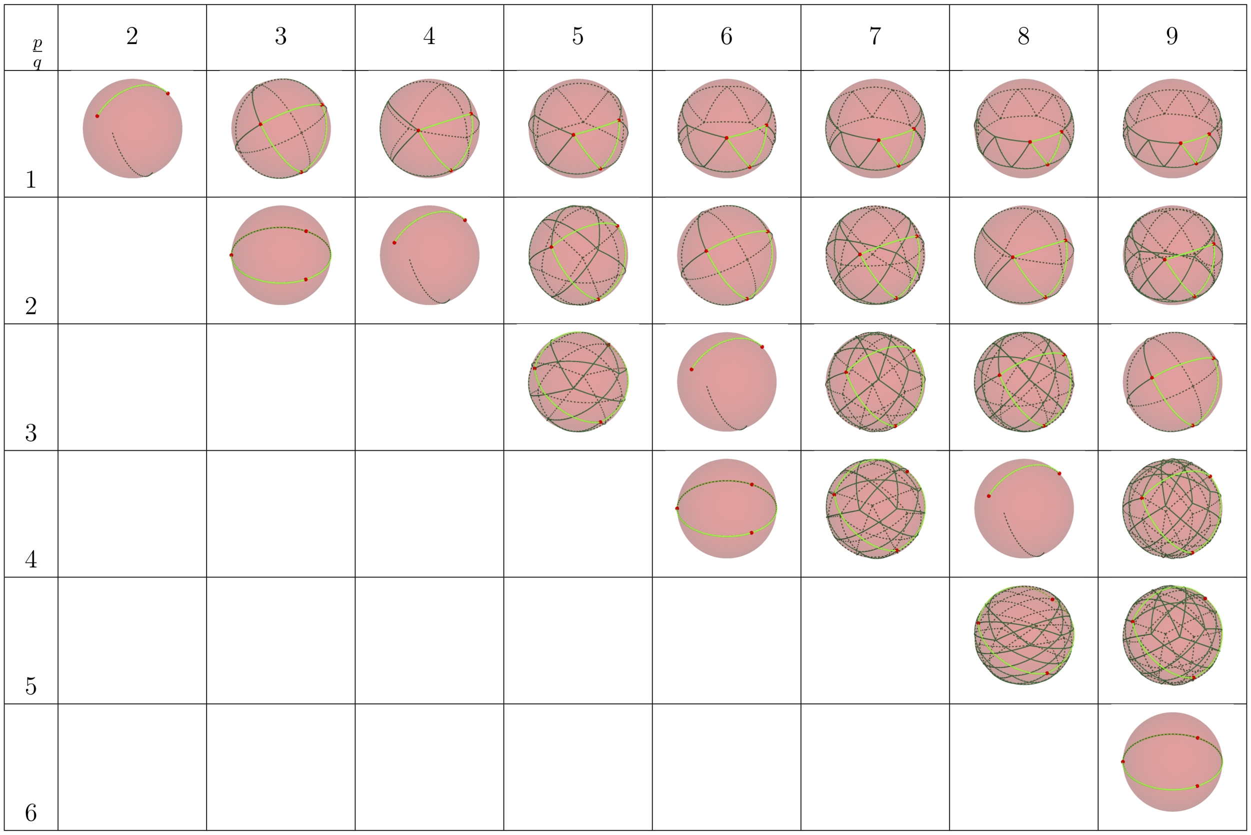

Figure 11: Configurations obtained with *GeoGebra* involving $\frac{p}{q}$-gons with $p > q$.

- if $B_1 \neq B_2$ then $\frac{p}{q} \neq \frac{1}{n}, n \in \mathbb{N}$;
- if $\frac{p}{q} = \frac{3}{2}$, the points B_1, B_2 and A_3 are coplanar and $|B_1B_2| = |B_2A_1| = |A_1B_2| = \frac{2\pi}{3}$, and we have the sphere divided in two hemispheres. However, this case corresponds to having A_1 on the arc $[B_1,B_2]$, which is not in consideration.
- the non trivial cases arise when $\frac{p}{q} > \frac{3}{2}$ and $\gcd(p, q) = 1$.

3. Results

Theorem 3.1. *Let p and q be natural numbers such as $\frac{p}{q} > \frac{3}{2}$ and $\gcd(p, q) = 1$. Let $k = \min\{q, p - q\}$ and denote respectively by v, e and t, the number of vertices, edges and faces of the spherical tiling $\widehat{\mathfrak{B}_{\frac{p}{q}}}$, associated to $\mathfrak{B}_{\frac{p}{q}}$. Then*

- $v = p(2k + q - 1)$,
- $e = 2p(2k + q - 1)$,
- $f = p(2k + q - 1) + 2$.

Proof. The orbits of the points A_1 and B_1, as defined above, by the group of rotations abut the z-axis through multiples of $2\pi/\frac{p}{q}$ generates two $\frac{p}{q}$ *spherical star-polygons*, Sp_T and Sp_D, about the points $(0, 0, 1)$ and $(0, 0, -1)$, respectively.

Denote by T_j and D_j the vertices of Sp_T and Sp_D, with $j \in \{1, \ldots, p\}$, respectively. These vertices of Sp_T and Sp_D are given by $T_j = Rot_{Oz}(B_1, (j-1)\frac{2\pi}{p})$ and $D_j = Rot_{Oz}(A_1, (j-1)\frac{2\pi}{p})$ with $j \in \{1, \ldots, p\}$. The configurations of Sp_T, and Sp_D are the same as those corresponding to $\frac{p}{q}$ and $\frac{p}{p-q}$. Let $k = \min\{q, p-q\}$. Thus, the number of vertices in Sp_T and Sp_D as part of $\widehat{\mathfrak{B}_{\frac{p}{q}}}$ is kp (see Figure 12).

Let us now see how to count the number of edges in Sp_T and Sp_D as part of $\widehat{\mathfrak{B}_{\frac{p}{q}}}$. Each arc T_iT_{i+q} (respectively D_iD_{i+q}) is divided into $2k-1$ arcs giving rise to $p(2k-1)$ edges. Thus, in total, Sp_T and Sp_D contribute with $2p(2k-1)$ edges to the edges of $\widehat{\mathfrak{B}_{\frac{p}{q}}}$.

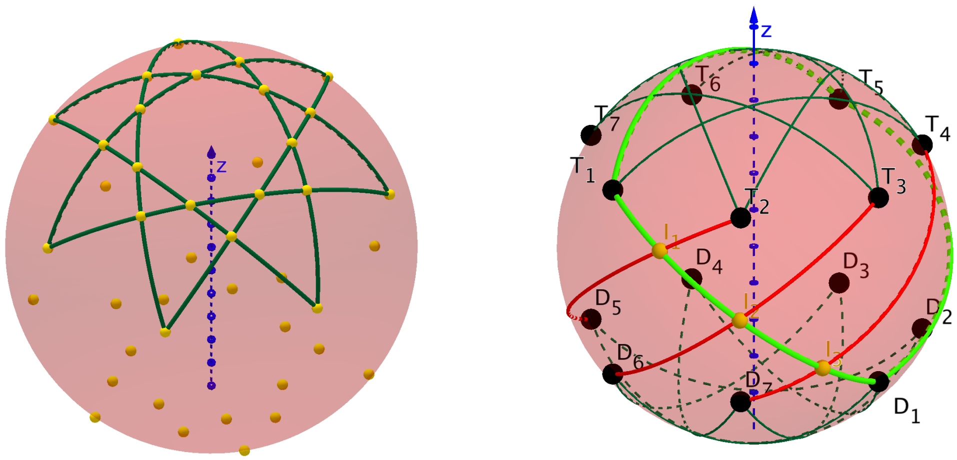

Figure 12: Vertices and cross points $\widehat{\mathfrak{B}_{\frac{p}{q}}}$.

The "lateral" edges[5] of $\widehat{\mathfrak{B}_{\frac{p}{q}}}$ joining the (external) vertices of Sp_T and Sp_D are the arcs corresponding to the orbit of the arcs T_1D_1 and D_1T_{1+q} by the cyclic group generated by the rotation of angle $\frac{2\pi}{p}$ about the z-axis. The arc T_1D_1 intersects the arcs $T_{1+j}D_{p-q+j}$ in $q-1$ cross points I_j with $j \in \{1, \ldots, q-1\}$. Therefore, the vertices T_1, D_1 and the cross points, $(I_j)_{j\in\{1,\ldots,q-1\}}$, define q edges $[T_1I_1], [I_1I_2], \ldots, [I_{j-1}I_j], [I_jD_1]$ of the $\widehat{\mathfrak{B}_{\frac{p}{q}}}$ tiling (see Figure 12). Thus the "lateral" net of $\widehat{\mathfrak{B}_{\frac{p}{q}}}$ has $p(q-1)$ vertices and pq edges.

Consequently $\widehat{\mathfrak{B}_{\frac{p}{q}}}$ has $v = p(2k+q-1)$ vertices, $e = 2p(2k+q-1)$ edges, and $f = p(2k+q-1)+2$ faces, being $(k-1)p$ triangles and $p(q+1)$ quadrilaterals. $\square$

Corollary 3.1.1. *If $\frac{p}{q} \in \mathbb{N}$ the family $\widehat{\mathfrak{B}_{\frac{p}{q}}}$ corresponds to the $\frac{p}{q}$-antiprismatic tilings.*

Theorem 3.2. *Let p and q be natural numbers such that $\gcd(p,q) = 1$ and $\frac{p}{q} > \frac{3}{2}$. Then the tilings $\widehat{\mathfrak{B}_{\frac{p}{q}}}$*

- *are invariants of the cyclic group C_p;*
- *if q is odd then the tilings have central symmetry;*
- *if q is even hen the tilings have reflection symmetry.*

Proof. The first and second statement are true having in consideration the construction of the band $\mathfrak{B}_{\frac{p}{q}}$ and the corresponding notation, given previously.
For the last statement it is enough to observe that

[5] In fact, the spherical segments that emerged between the vertices of Sp_T and Sp_D correspond to a helical polygon [8].

- the vertices $A_i \in 1, \ldots p$ are on the orthogonal bisector of the arc segment B_iB_{i+1}. Thus, when q is even, the projections of the orbits of A_i and B_i in the plane $z = 0$ coincide;
- the edges of the lateral net whose endpoints are not (external) vertices of Sp_T and Sp_D form an even number of edges of $\widehat{\mathfrak{B}_{\frac{p}{q}}}$ defining $q - 1$ vertices of this tiling. □

4. Exploring spherical tilings with GeoGebra

Here, we explore possible conjectures starting from a spherical triangle and its orbit under a local action of spherical reflections. We obtain a determined pattern by constructing a spherical triangle using the tools described in Section 2 and reflecting it in the planes containing its sides. We implemented this procedure in a *GeoGebra* application entitled "edge to edge".

Using this application and iterating it, we get a sequence of spherical patterns as the one illustrated in Figure 13a. Since the initial triangle is not fixed, it is expected that some of these patterns will end up in monohedral spherical tilings (see Figure 13b).

In Figure 13b we illustrated this process beginning with the (fixed) spherical triangle ($\pi/2$, $\pi/2$, $\pi/3$). As expected, we end up with the hexagonal bypyramidal tiling. Using the same strategy but starting with the family of spherical triangles of angles ($\pi/2$, $\pi/2$, $2\pi/n$) we end up with the family of n-gons bypiramidal tiling.

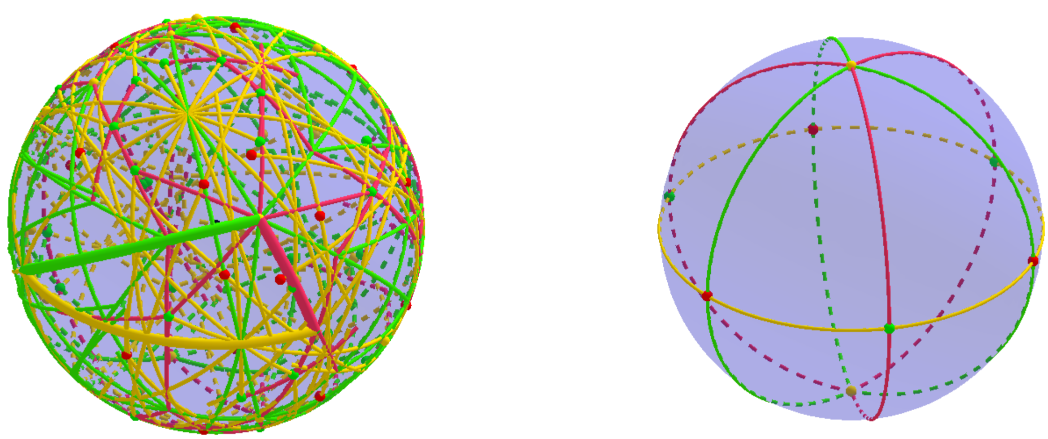

(a) Angles $\pi/5$, $2\pi/5$, and $3\pi/5$

(b) Angles $\pi/2$, $\pi/2$, and $\pi/3$

Figure 13: Spherical monohedral tilings, evolution to bi-pyramids tiling.

Starting with the spherical triangle with angles $\pi/3$, $\pi/4$, and $\pi/2$ and using the same technique, we end up with a spherical tiling with octahedral symmetry which corresponds to a polyhedron with 48 faces, the Catalan polyhedron *disdyakis dodecahedron* (see Figure 14a).

The spherical triangle with angles $\pi/5$, $\pi/3$, and $\pi/2$ gives rise to a spherical tiling with 120 congruent scalene triangles (see Figure 14b), with icosahedral symmetry, which corresponds to the Catalan polyhedron *disdyakis triacontahedron*.

Using the spherical triangle of angles $\pi/3$, $3\pi/4$, and $\pi/4$, we can obtain a tiling by 12 congruent scalene spherical triangles, that corresponds to a non-convex polyhedron with 12 triangular faces, 8 vertices and 18 edges (see Figure 14c). Continuing this process, we end up always with a spherical tiling in which the starting triangle is not a tile of the achieved tiling but it is decomposed into tiles of the new tiling.

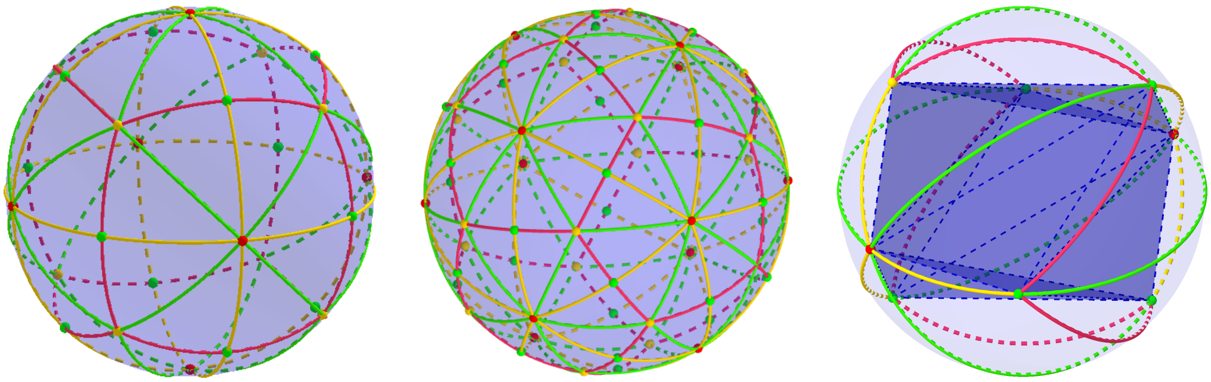

(a) Angles $\pi/3$, $\pi/4$, and $\pi/2$ (b) Angles $\pi/5$, $\pi/3$, and $\pi/2$ (c) Angles $\pi/3$, $3\pi/4$, and $\pi/4$

Figure 14: Spherical monohedral tilings by triangles.

The explorations carried out so far present some interesting results that need to be strengthened. It seems that, using Schwarz triangles, this procedure seems to be able to provide a dynamic illustration of the polyhedral kaleidoscopes studied by Coxeter [8].

5. Conclusions

We have presented several new *GeoGebra* tools that may be used to explore spherical geometry and to explore spherical tilings. An important advantage of these applications is the interactivity and the visualisation of the created objects, promoting conjectures and the respective formal proofs. The conjectures can also be tested by the *GeoGebra* CAS capabilities.

Acknowledgements

This work was supported in part by the Portuguese Foundation for Science and Technology (FCT – Fundação para a Ciência e a Tecnologia), through CIDMA – Centre for Research and Development in Mathematics and Applications, within the project UID/MAT/04106/2013. Special thanks to João Jorge Ribeiro Soares Gonçalves de Araújo for helpful comments and for reading this paper.

References

[1] D. Austin, W. Dickinson: *Spherical easel. A spherical drawing program.* 2002–2009, `http://merganser.math.gvsu.edu/easel/` (visited 10/05/2018).

[2] C. Beltrán: *A facility location formulation for stable polynomials and elliptic Fekete points.* Found. Comput. Math. **15**.1, 125–157 (2015), `https://doi.org/10.1007/s10208-014-9213-` (visited 10/05/2018).

[3] J.S. Brauchart, P.J. Grabner: *Distributing many points on spheres: minimal energy and designs.* J. Complexity **31**.3, 293–326 (2015), `http://www.sciencedirect.com/science/article/pii/S0885064X15000205` (visited 10/05/2018).

[4] A.M. d'Azevedo Breda, J.M. Dos Santos: *A new class of monohedral pentagonal spherical tilings with GeoGebra.* Port. Math. **74**.3, 257–266 (2018), `https://ria.ua.pt/bitstream/10773/22148/1/PM_74-3_06{\%}20257.pdf` (visited 10/05/2018).

[5] A.M. d'Azevedo Breda, J.M. Dos Santos: *Dihedral antiprismatic spherical Tilings*. 2018, https://ggbm.at/vybwsjm4 (visited 25/11/2018).

[6] A.M. d'Azevedo Breda, J.M. Dos Santos: *Evolution of nets of equilateral spherical triangles*. 2018, https://ggbm.at/z6qsuwzj (visited 25/11/2018).

[7] A.M. Azevedo Breda: *A class of tilings of S2*. Geom. Dedicata **44**.3, 241–253 (1992), https://doi.org/10.1007/BF00181393 (visited 10/05/2018).

[8] H.S.M. Coxeter: *Regular complex polytope*. Cambridge University, 1974.

[9] H.L. Davies: *Packings of spherical triangles and tetrahedra*. In: Proc. Colloquium on Convexity, Copenhagen 1965, 1967, pp. 42–51.

[10] R.J. MacG. Dawson: *An isosceles triangle that tiles the sphere in exactly three ways*. Discrete Comput. Geom. **30**.3, 459–466 (2003), https://link.springer.com/article/10.1007/s00454-003-2777-0 (visited 10/05/2018).

[11] R.J. MacG. Dawson: *Some New Tilings of the Sphere with Congruent Triangles*. In: *Renaissance Banff: Mathematics, Music, Art, Culture*, Bridges Conference 2005, pp. 489–496, https://archive.bridgesmathart.org/2005/bridges2005-489.pdf (visited 10/05/2018).

[12] R.J. MacG Dawson: *Tilings of the sphere with isosceles triangles*. Discrete Comput. Geom. **30**.3, 467–487 (2003), https://link.springer.com/article/10.1007/s00454-003-2846-4 (visited 10/05/2018).

[13] R.J. MacG. Dawson, B. Doyle: *Tilings of the sphere with right triangles I: the asymptotically right families*. Electron. J. Combin. **13**.2, 48 (2006), http://emis.ams.org/journals/EJC/Volume_13/PDF/v13i1r48.pdf (visited 10/05/2018).

[14] B. De Nijs et al.: *Entropy-driven formation of large icosahedral colloidal clusters by spherical confinement*. Nature materials **14**.1, p. 56 (2015), web.science.uu.nl/SCM/Articles/2015/de{\%}20Nijs_NatureMater_2015.pdf (visited 10/05/2018).

[15] M. Deza et al.: *Fullerenes as tilings of surfaces*. J. Chem. Inf. Comput. Sci. **40**.3, pp. 550–558 (2000), http://citeseerx.ist.psu.edu/viewdoc/download?doi=10.1.1.105.5973&rep=rep1&type=pdf (visited 10/05/2018).

[16] M.V. Diudea, C.L. Nagy: *Periodic nanostructures*. Vol. 7, Springer Science & Business Media, 2007.

[17] J. Erdös: *Sphaerica: Interactive Spherical Geometry Software*. In G.W. Hart, R. Sarhangi (eds.): *Proceedings of Bridges 2010: Mathematics, Music, Art, Architecture, Culture*, Phoenix/Arizona: Tessellations Publishing, 2010, pp. 443–446, http://archive.bridgesmathart.org/2010/bridges2010-443.pdf (visited 10/05/2018).

[18] M. Hohenwarter: *Ein Softwaresystem für dynamische Geometrie und Algebra der Ebene*. MA thesis Salzburg: Paris Lodron University, 2002, http://archive.geogebra.org/static/publications/diplomarbeit_geogebra.pdf (visited 10/05/2018).

[19] M. Hohenwarter: *GeoGebra. Geometry and Algebra Software*. 2002, https://www.geogebra.org/ (visited 10/05/2018).

[20] M. Hohenwarter, K. Fuchs: *Combination of dynamic geometry, algebra and calculus in the software system GeoGebra*. In: Computer Algebra Systems and Dynamic Geometry Systems in Mathematics Teaching Conference 2004, http://archive.geogebra.org/static/publications/pecs_2004.pdf (visited 10/05/2018).

[21] A.A. Rezaei: *Polygonal tiling of some surfaces containing fullerene molecules*. Iran. J. Math. Chem. **5**.2, 99–105 (2014), http://ijmc.kashanu.ac.ir/article_7375_490966fb9747f786985dfc15d4bc6a1a.pdf (visited 10/05/2018).

[22] A.A. Rezaei: *Tiling Fullerene Surface with Heptagon and Octagon*. Fullerenes, Nanotubes and Carbon Nanostructures **23**.12, 1033–1036 (2015), https://doi.org/10.1080/1536383X.2015.1057817 (visited 10/05/2018).

[23] E.B. Saff, A.B.J. Kuijlaars: *Distributing many points on a sphere*. Math. Intelligencer **19**.1, 5–11 (1997), https://perswww.kuleuven.be/~u0017946/publications/Papers97/art97a-Saff-Kuijlaars-MI/Saff-Kuijlaars-MathIntel97.pdf (visited 10/05/2018).

[24] D.M.Y. Sommerville: *VI. – Division of Space by Congruent Triangles and Tetrahedra*. Proc. Roy. Soc. Edinburgh **43**, 85–116 (1924).

[25] G. Stahl: *Adventures in dynamic geometry*. Lulu.com 2018, http://gerrystahl.net/elibrary/topics/topics.pdf (visited 17/11/2018).

[26] L. Szilassi: *A Bolyai geometria – szemléletesen*. 2018, https://www.geogebra.org/m/NSQ9meGe (visited 17/11/2018).

[27] Yuan-Zhi Tan et al.: *Carbon arc production of heptagon-containing fullerene [68]*. Nature Commun. **2**, ncomms1431, https://www.nature.com/articles/ncomms1431.pdf (visited 10/05/2018).

[28] GeoGebra Team. Tutorial: *Custom Tools and Customizing the Toolbar,* 2016Ű, https://wiki.geogebra.org/en/Tutorial:Custom_Tools_and_Customizing_the_Toolbar (visited 10/05/2018).

[29] Y. Ueno, Y. Agaoka: *Tilings of the 2-dimensional sphere by congruent right triangles*. In: Memoirs of the Faculty of Integrated Arts and Sciences, Hiroshima University. IV, Science reports: studies of fundamental and environmental sciences 22 (1996), pp. 1–23, http://ir.lib.hiroshima-u.ac.jp/files/public/0/673/20141016120323365034/KJ00000197303.pdf (visited 10/05/2018).

[30] Y. Ueno, Y. Agaoka et al.: *Classification of tilings of the 2-dimensional sphere by congruent triangles*. Hiroshima Math. J. **32**.3, 463–540 (2002), http://www.math.sci.hiroshima-u.ac.jp/hmj/v32.3/P463-540.PDF (visited 10/05/2018).

[31] Zhi Wang et al.: *Assembly of silver Trigons into a buckyball-like Ag180 nanocage*. In: Proceedings of the National Academy of Sciences 114.46 (2017), pp. 12132–12137, http://www.pnas.org/content/pnas/114/46/12132.full.pdf (visited 10/05/2018).

Received May 10, 2018; final form November 30, 2018